AD-A132 624 THE CONVERSION OF OFF-VERTICAL OBSERVATIONS OF TOTAL ELECTRON CONTENT INT..(U) AIR FORCE GEOPHYSICS LAB HANSCOM AFB MA L F MCNAMARA 06 APR 83 AFGL-TR-83-0092 1/1

UNCLASSIFIED F/G 4/1 NL

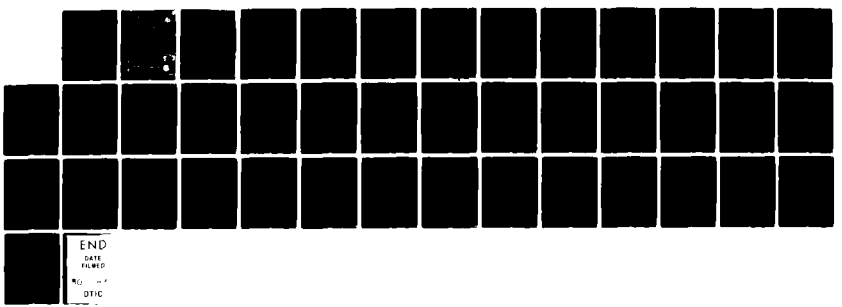

END

DATE FILMED

DTIC

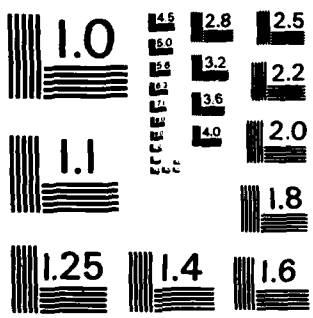

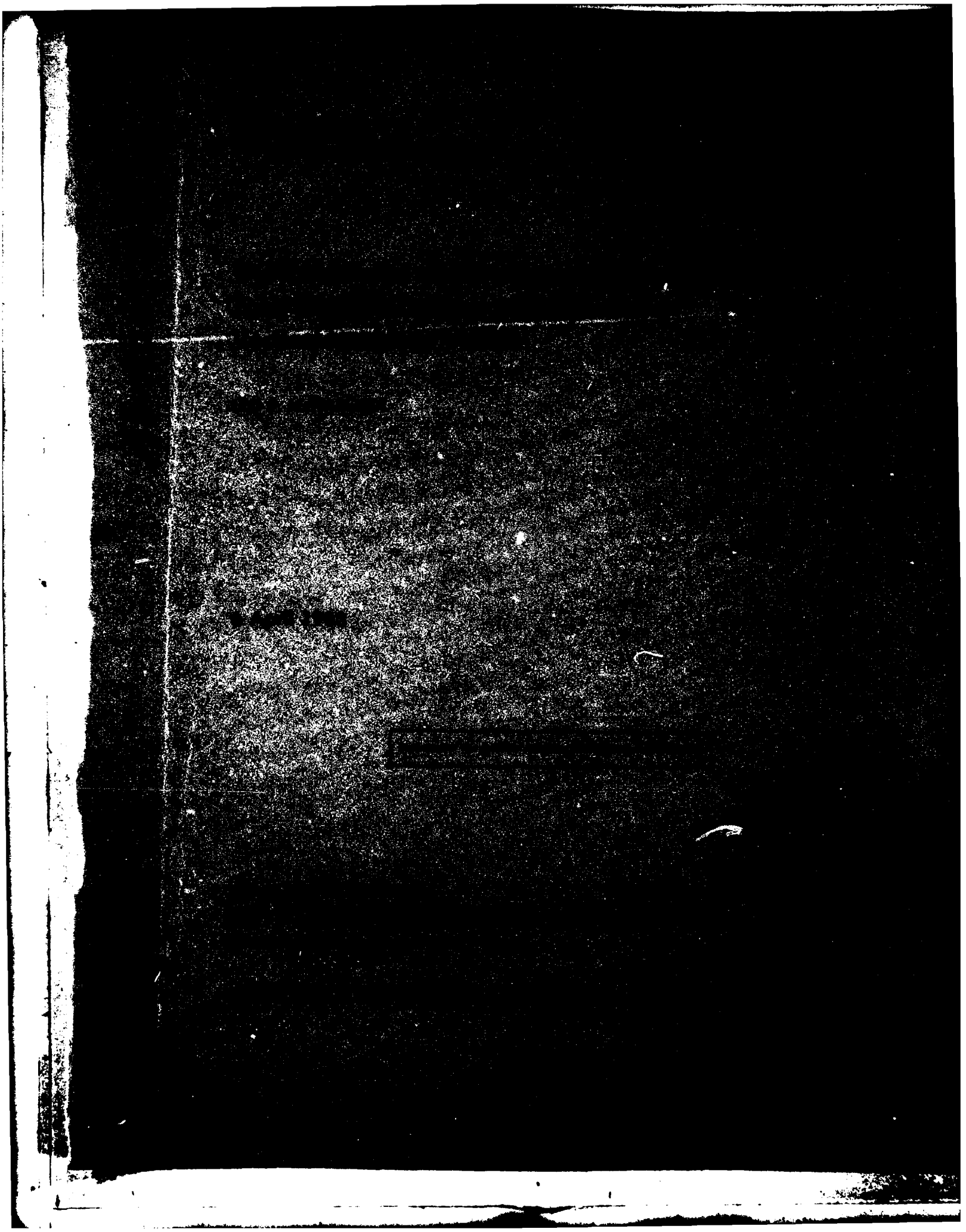

This report has been reviewed by the ESD Public Affairs Office and is releasable to the National Technical Information Service.

This Technical Report has been reviewed and is approved for publication.

Alva T. Stair, Jr.

DR. ALVA T. STAIR, JR.
Chief Scientist

Qualified requesters may obtain additional copies from the Defense Technical Information Center. All others should apply to the National Technical Information Service.

Unclassified

SECURITY CLASSIFICATION OF THIS PAGE (When Data Entered)

REPORT DOCUMENTATION PAGE		READ INSTRUCTIONS BEFORE COMPLETING FORM
1. REPORT NUMBER AFGL-TR-83-0092	2. GOVT ACCESSION NO.	3. RECIPIENT'S CATALOG NUMBER
4. TITLE (and Subtitle) THE CONVERSION OF OFF-VERTICAL OBSERVATIONS OF TOTAL ELECTRON CONTENT INTO EQUIVALENT VERTICAL-INCIDENCE VALUES		5. TYPE OF REPORT & PERIOD COVERED Scientific. Interim. 6. PERFORMING ORG. REPORT NUMBER ERP, No. 832
7. AUTHOR(s) Leo F. McNamara		8. CONTRACT OR GRANT NUMBER(s)
9. PERFORMING ORGANIZATION NAME AND ADDRESS Air Force Geophysics Laboratory (PHY) Hanscom AFB Massachusetts 01731		10. PROGRAM ELEMENT, PROJECT, TASK AREA & WORK UNIT NUMBERS 46430901 62101F
11. CONTROLLING OFFICE NAME AND ADDRESS Air Force Geophysics Laboratory (PHY) Hanscom AFB Massachusetts 01731		12. REPORT DATE 6 April 1983 13. NUMBER OF PAGES 41
14. MONITORING AGENCY NAME & ADDRESS(if different from Controlling Office)		15. SECURITY CLASS. (of this report) Unclassified 15a. DECLASSIFICATION DOWNGRADING SCHEDULE

16. DISTRIBUTION STATEMENT (of this Report)

Approved for public release; distribution unlimited.

17. DISTRIBUTION STATEMENT (of the abstract entered in Block 20, if different from Report)

18. SUPPLEMENTARY NOTES

NRC/AFSC Senior Research Associate on leave from the Australian Ionospheric Prediction Service, P.O. Box 702, Darlinghurst 2010, Australia.

19. KEY WORDS (Continue on reverse side if necessary and identify by block number)

Conversion of slant to vertical TEC
TEC from high-orbit satellites
TEC slant path corrections

20. ABSTRACT (Continue on reverse side if necessary and identify by block number)

Observations of total electron content along off-vertical paths are normally converted into an equivalent vertical incidence total content before their application in studies of the ionosphere or in communications predictions. The errors in this conversion have been studied using a numerical model of the ionosphere. The errors are found to vary with the azimuth and elevation of the satellite, the altitude at which the conversion is made, the presence of ionospheric gradients along the ground-satellite path, and with the well-known variations of the ionosphere itself. For elevation angles of 20° or greater,

DD FORM 1 JAN 73 1473 EDITION OF 1 NOV 65 IS OBSOLETE

Unclassified

SECURITY CLASSIFICATION OF THIS PAGE (When Data Entere

20. (Contd)

the relative errors are usually less than about 10% and often less than about 5%, for a wide range of conditions. Errors of up to 20% are obtained for equatorial stations and for stations near the high latitude trough, especially for low angles of elevation.

Preface

The author wishes to acknowledge Mr. J.A. Klobuchar for his guidance and many useful discussions throughout this study, and Patricia Doherty for her support with the computer programming.

Contents

Illustrations

Tables

The Conversion of Off-Vertical Observations of Total Electron Content Into Equivalent Vertical-Incidence Values

1. INTRODUCTION

Observations of the total electron content (TEC) of the ionosphere have been made over the past two decades and have been used extensively to improve our knowledge of the ionosphere and to correct for its effects on signals propagating through it. Most observations of TEC are made using a satellite not directly overhead of the observer, yielding what can be called TEC_s, the total electron content along a slant path. To be more readily understood and more useful in studies of the ionosphere and for updating models of the ionosphere for operational purposes, these observations must be converted to a vertical incidence value, TEC_v, corresponding to a vertical profile at some point in the ionosphere along the ground-satellite path. This conversion is by necessity an approximate procedure, the limits of which will be described in this report.

An approximate relationship between TEC_s and TEC_v may be established by a little geometry, as illustrated in Figure 1. We have

$$TEC = \int_0^{HS} N \, ds \qquad (1)$$

(Received for publication 4 April 1983)

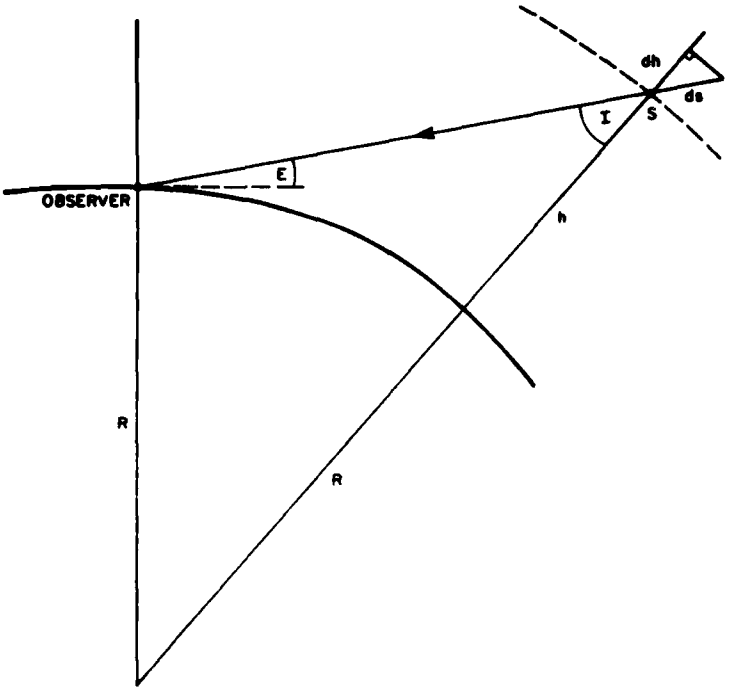

Figure 1. Observer-Satellite Geometry. The satellite is at an altitude h; the elevation angle at the ground is E; and the angle of incidence at the satellite is I

where the integration is performed along the observer-satellite path and HS is the height of the satellite. Using Figure 1, it follows that

$$TEC_s = \int_0^{HS} N \sec I \, dh \tag{2}$$

where the integration is now performed in the radial direction and I is the angle of incidence of the ray. An expression for I can be deduced from Figure 1, using the sine rule:

$$\sec I(h, E) = \left\{ 1 - \left(\frac{R \cos E}{R + h} \right)^2 \right\}^{-1/2} \tag{3}$$

where E is the angle of elevation at the surface of the earth.

With the loss of some accuracy, sec I may be removed from the integrand and replaced in Eq. (2) by an average value, $\overline{\sec I}$:

$$TEC_s = \overline{\sec I} \int_0^{HS} N \, dh \, . \qquad (4)$$

The integrand on the right hand side of Eq. (3) is just the vertical incidence total content, TEC_v, so we have

$$TEC_s = \overline{\sec I} \, TEC_v \, . \qquad (5)$$

This is the required equation relating slant- and vertical-incidence values of TEC.

The use of an average value of sec I, with sec I being evaluated at an appropriate altitude h_I, implicitly assumes that the integrand N(h) sec I(h, E) peaks fairly sharply at h_I. Since sec I is a slowly varying function of h, the integrand in fact peaks around the peak of the N(h) distribution and h_I should be set to an altitude near hmF2. The error resulting from the use of Eq. (5) will depend to an important extent on the choice of h_I.

Traditionally, most observations of TEC have been made using the Faraday rotation technique and geostationary satellites. For these observations, the observed values of TEC correspond to the total content up to 2000 km, and are applied to the ionospheric point where the ground-satellite path cuts an altitude of 400 to 420 km. This procedure was recommended by Titheridge.[1] The altitude of 420 km, the "mean field height", is appropriate under such conditions because the amount of Faraday rotation depends on the earth's magnetic field, as well as on the ionosphere and geometry of the ray path.

The same choice of altitude is not necessarily appropriate for the conversion of TEC_s to TEC_v when different measurement techniques, not affected by the earth's magnetic field, are employed. Llewellyn and Bent,[2] for example, set h_I equal to hmF2, the height of the F2 layer peak, for their model studies.

For reasonably high angles of elevation (say 30 to 90°), the exact altitude at which sec I is calculated (and which is used to determine the ionospheric point with which TEC_v is to be associated) is not important because TEC_s is not a sensitive function of this altitude. However for very low angles of incidence, such as can be encountered using polar-orbiting satellites and high-latitude ground stations looking at geostationary satellites, sec I varies rapidly with height and the value of TEC_v determined from a value of TEC_s depends strongly on the choice of height at which sec I is evaluated.

---

1. Titheridge, J. E. (1972) Determination of ionospheric electron content from the Faraday rotation of geostationary satellite signals, Planetary and Space Science, 20(3):353-370.

2. Llewellyn, S. K., and Bent, R. B. (1973) Documentation and Description of the Bent Ionospheric Model, AFCRL-TR-73-0657, AD 772733.

A second problem encountered with low elevation angles is that the trans-ionospheric path is so long that horizontal gradients become important and the simplifying assumptions on which Eq. (5) are based no longer apply.

This report therefore investigates the range of validity of Eq. (5) for low elevation angles. The errors in Eq. (5) are studied as a function of station location, azimuth, elevation, local time, season, and solar activity, as well as elevation angle. For those regions in which large errors are encountered, Eq. (5) should not be used. The most appropriate altitude at which sec I should be evaluated is also studied.

Section 2 describes the numerical methods used in this analysis. Section 3 discusses the errors associated with the use of different values of h_I and the most appropriate values to choose. The conversion errors obtained using Eq. (5) are discussed in Sections 4, 5, and 6 for typical low, high, and mid-latitude stations, while Section 7 discusses the errors for a chain of stations at 75° W. The cases studied are not exhaustive, and are meant to be representative only. More detailed and specific results may be obtained by running the computer program SLANTEC which is available from the author. The results are summarized in Section 8.

2. METHOD OF ANALYSIS

In order to determine the errors in TEC_s to TEC_v conversion, it is necessary to have accurate values for each. In general, this can be done only by model studies, since simultaneous observations of TEC_s and TEC_v are very difficult to arrange. The model of the ionosphere which is used must be as faithful a representation of the real ionosphere as possible, especially in regard to the variation of electron density with height. The Bent model[2] is such a model, having been constructed so as to reproduce TEC observations over a wide range of conditions. Consequently, this model has been used in the present study.

The calculation of TEC_v for a given location is readily achieved using the techniques used by Bent—calculate foF2 and hmF2 using spherical harmonic expansions; determine the corresponding vertical N(h) profile using an empirical model; integrate the (analytic) vertical N(h) profile to obtain TEC_v.

The calculation of TEC_s, on the other hand, is more complex because the integration is no longer analytic and must be replaced by a numerical integration. We have

$$TEC_s = \int_0^{HS} N(h, \theta) \sec I(h, E)\, dh \qquad (6)$$

where (a) θ denotes that N can change with latitude and longitude, (b) I is the angle of the incidence at the height h, corresponding to the elevation angle E, and (c) the integration is performed from the ground (h = 0) to the satellite (h = HS).

Equation (6) can be replaced by

$$TEC_s = \sum_{i=1}^{M} N_i \sec I_i w_i \tag{7}$$

that is, by an M-point quadrature with the integrand being evaluated at the heights h_i and with quadrature weights w_i. The values of h_i depend on the quadrature method and its order, and also on the limits of the height integration. We have chosen to use Gauss-Legendre quadrature (for example, Abramowitz and Stegun)[3] of different orders. The quadrature points and weights for this method correspond to integration limits of -1 to +1 so the method must be generalized for use with limits a to b. This is achieved by changing the integration variable:

$$I = \int_a^b f(y)\, dy . \tag{8}$$

Define

$$y = \frac{b - a}{2} x + \frac{b + a}{2} \tag{9}$$

then

$$\begin{aligned} I &= \int_{-1}^{+1} f[y(x)] \frac{b - a}{2} dx \\ &= \frac{b - a}{2} \int_{-1}^{+1} f[y(x)]\, dx \\ &= \frac{b - a}{2} \sum_{i=1}^{M} w_i f[y(x_i)] . \end{aligned} \tag{10}$$

The x_i and w_i are the Gaussian quadrature points and weights, $y(x_i)$ is evaluated using Eq. (9) and f is evaluated at $y(x_i)$. In the present example, f = Nsec I.

3. Abramowitz, M., and Stegun, I. A. (1964) Handbook of Mathematical Functions. NBS Applied Mathematics Series No. 55, U.S. Govt. Printing Office, Washington, D. C.

In practice, the value of TEC_s obtained by numerical integration will have some error, the size of which will depend on the order of integration chosen. The error will decrease as the order increases, but the computation time will increase, so it is necessary to choose as low an order as possible, commensurate with the desired accuracy.

The required order of integration may be reduced by working in terms of the error itself. This error is defined as

$$\text{ERROR} = \sec I_v \cdot TEC_v - TEC_s \tag{11}$$

and can be written as

$$\text{ERROR} = \sec I_v \sum_{i=1}^{M} w_i (N_v)_i - \sum_{i=1}^{M} w_i (N \sec I)_i$$

$$= \sum_{i=1}^{M} w_i \left\{ \sec I_v \cdot (N_v)_i - (\sec I \cdot N)_i \right\} . \tag{12}$$

In the first term, $\sec I_v$ is a constant, N_v is the vertical profile passing through the point at which $\sec I_v$ is calculated, and is evaluated at each of the M quadrature heights. In the second term, N is the vertical profile passing through each quadrature point along the integration path. sec I and N are both evaluated at each quadrature height.

The required order of integration may be further reduced by noting that the error term changes sign at the height at which $\sec I_v$ is evaluated. Consequently, it is more accurate to use two ranges of integration, HL to h_I and h_I to HU, where HL and HU are the lower and upper limits of the full integration.

Once the error term has been calculated, the correct value of TEC_s can be obtained from Eq. (11). Most of the discussion of errors in this report is concerned with the error

$$\% \text{ error} = \frac{\sec I_v \cdot TEC_v - TEC_s}{TEC_s} \times 100$$

$$= \frac{\text{ERROR}}{TEC_s} \times 100 .$$

This error is positive if the simple sec I approximation yields too high a result, and vice versa.

Figure 2 shows some typical integrands (terms) of Eq. (12). It can be seen that the error changes sign at h_I, which is 420 km in this case. The limits of

integration are 200 and 2000 km and 8-point quadrature is used in both integration ranges. Since the error is an oscillating function of height, some cancellation occurs, the over-all error depending on the extent of the cancellation. The upper limit of integration could be lowered to 1200 km without introducing any appreciable errors, since the contribution to the integral from 1200 to 2000 km is negligible.

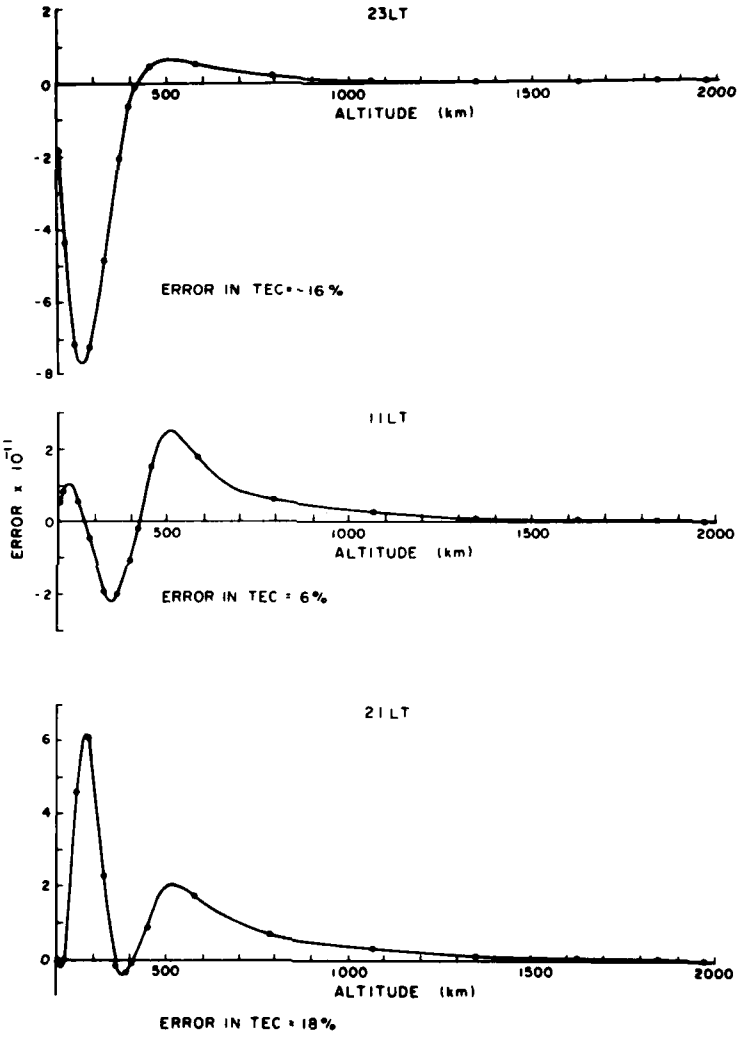

Figure 2. Variation of the Error Integrand With Integration Height for Three Local Times (Kwajalein, March, R= 100, h_I = 420 km, Elevation = 10°)

3. SELECTION OF THE HEIGHT h_I

The errors in the conversion of TEC_s to TEC_v are found to be a complicated function of all variables—station location, solar activity, month, time of day, azimuth, elevation, h_I—and these variations are inter-dependent. Consequently, in order to investigate each different variation it is necessary to hold all other parameters constant or to average the errors over the ranges of these other parameters.

The first variation which must be considered is that of the errors versus the choice of h_I. Ideally, a single value of h_I should lead to the smallest possible errors under all circumstances. However, this is found to be not the case.

The conversion error has been studied as a function of h_I, for three stations, four months of the year, and for low and high solar activity. The stations chosen are representative low-latitude (Kwajalein), mid-latitude (Cape Canaveral), and high-latitude (Goose Bay) stations. Values of h_I have been taken from 320 to 460 km, in steps of 20 km, and values related to hmF2 have also been used; hmF2 plus 0, 50, 100 and 150 km. The use of a fixed altitude, rather than one related to hmF2, seems preferable because it obviates the need for a knowledge (most likely from an ionospheric model) of hmF2. On the other hand, however, the appropriate value of h_I would be expected to be related to hmF2 and have similar diurnal and other variations.

Table 1 shows the RMS errors for Kwajalein, Cape Canaveral and Goose Bay, for March, June, September, and December, and for R_{12} = 100 and 10 (corresponding fluxes of 150 and 75). Only those errors necessary to define the pattern have been calculated. The errors have been averaged over the day (00, 06, 12, 18 UT), azimuth (0°, 90°, 180°, 270°) and elevation angle (0°, 10°, 20°, 30°). The entries underlined in the table are the minimum values for each case. Clearly, there is no single height, h_I, which should be used in all circumstances. For Cape Canaveral, the error minimizes at 380 ± 20 km, while for Kwajalein it minimizes at 400 ± 20 km (approximately). For Goose Bay, low solar activity, the error minimizes at 380 ± 20 km, but for high solar activity, there is no obvious best choice of h_I. (This indicates the presence of a systematic error in the conversion which cannot be overcome by using a suitable h_I).

When h_I is related to hmF2, the errors are least for hmF2 + 50 or hmF2 + 100 km, but have not been investigated in great detail. This result is readily explained by noting that the centroid of the Bent N(h) profile is about 50 km above hmF2. Two things can be noted about the results for h_I related to hmF2:

Table 1. RMS Percentage Conversion Errors Averaged Over Elevation Angle (0, 10, 20, 30°), Azimuth (0, 90, 180, 270°) and Over the Day (0, 06, 12, 18 UT). The errors are given for different values of h_I, four months, two levels of solar activity and for stations at three latitudes. The underlined values are the minimum errors as a function of h_I, for each set of h_I (hmF2 · 0, 50, 100, 150 km; 320-460 km)

Station	Month	R	HM	50	100	150	320	340	360	380	400	420	440	460
Kwajalein	MAR	100	9.3	6.3	6.3	8.0	12.1	10.4	9.2	8.4	7.9	7.7	7.8	
	JUN		9.5	5.8	5.3	7.2	12.7	10.9	9.3	8.2	7.5	7.1	7.1	
	SEP		8.8	5.4	5.1	7.1		10.5	9.1	8.0	7.2	6.8	6.9	7.2
	DEC		8.8	4.8	5.8	8.6	10.9	9.0	7.6	6.8	6.8	7.1	7.7	
	MAR	10	10.7	6.4	5.8	8.0		7.5	7.0	6.9	7.1	7.8	8.6	9.6
	JUN		11.9	7.0	4.9	6.1		7.7	6.5	5.9	5.9	6.3	6.9	7.8
	SEP		12.1	7.0	5.6	7.8		8.0	7.0	6.6	6.8	7.6	8.5	9.6
	DEC		10.3	5.4	4.4	7.0	6.5	5.4	5.0	5.3	6.1	7.2	8.2	
Cape Canaveral	MAR	100	6.0	2.8	3.6	6.0	5.6	4.2	3.2	2.9	3.2	4.0	4.9	
	JUN		6.5	3.3	3.3	5.5	7.3	5.7	4.2	3.0	2.3	2.4	3.1	
	SEP						6.0	4.5	3.3	2.7	2.8	3.5	4.4	
	DEC							3.6	2.9	3.0	3.9	4.9	6.1	
	MAR	10	9.9	4.8	2.1	4.1	5.7	4.1	2.9	2.5	2.9	3.9	4.9	
	JUN		9.4	5.1	2.7	3.7	6.1	4.6	3.4	2.6	2.5	3.0	3.8	
	SEP						6.2	4.6	3.3	2.7	2.9	3.7	4.7	
	DEC							3.6	2.7	2.8	3.6	4.7	5.8	
Goose Bay	MAR	100	12.1	3.4	4.0	3.5		11.5	9.5	7.8	6.2	5.0	4.2	3.8
	JUN							10.0	8.4	6.9	5.5	4.3	3.3	2.5
	SEP							9.4	7.7	6.2	4.9	3.8	3.2	3.0
	DEC							12.6	10.2	8.2	6.6	5.4	5.0	5.2
	MAR	10	8.7	4.2	2.2	4.1		3.6	2.4	1.9	2.4	3.3	4.3	5.3
	JUN							4.3	3.0	1.9	1.6	2.1	3.0	4.0
	SEP							3.2	2.2	2.0	2.5	3.4	4.4	5.4
	DEC							2.4	2.2	2.9	4.0	5.1	6.2	7.3

(1) For Kwajalein, at least, the RMS errors are lower for h_I = hmF2 + 100 km than for h_I = 400 km. This indicates that the former would be preferable, provided that hmF2 were known reliably.

(2) The choice of hmF2 + 50 or + 100 km is usually far superior to the use of hmF2 itself, which is the procedure adopted by Llewellyn and Bent.[2]

The diurnal variation of the error for values of h_I of 400 km and hmF2 + 50 km is shown in Figure 3, for four azimuths. The results are for Kwajalein, March, R = 100, elevation angle equal to 10°. The largest errors are obtained looking north and south (the reasons for this are explained in Section 4) and are greater in general for h_I = 400 km. These errors tend to be positive during the day (h_I is too low) and negative at night (h_I too high). When h_I is allowed to follow the variation of hmF2, the errors generally decrease below those for h_I = 400 km and to have a less definite diurnal variation.

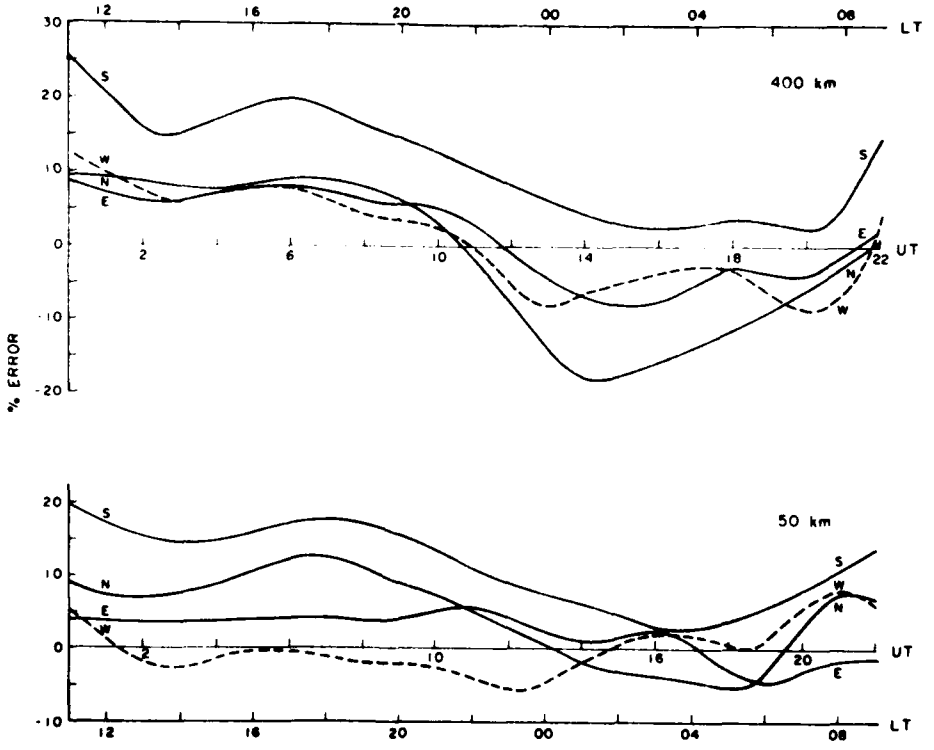

Figure 3. Diurnal Variation of the Conversion Error for North, South, East, and West Azimuths, for h_I = 400 km and hmF2 + 50 km (Kwajalein, March, R = 100, Elevation = 10°)

Figure 4 illustrates how the error depends on the choice of h_I, for four azimuths and four local times. The error is plotted as a function of elevation angle and the results are for Kwajalein, March, R = 100. It can be seen that the error is a complicated function of azimuth, elevation, local time, and h_I, at least for low elevation angles, but it is the variation of error with h_I which is of immediate concern here. This is especially important for low elevation angles, whereas for higher elevation angles (greater than 20° or 30°) the errors are fairly insensitive to the choice of h_I. Only for low elevation angles is it really necessary to attempt to minimize the errors by choosing the "best" value of h_I.

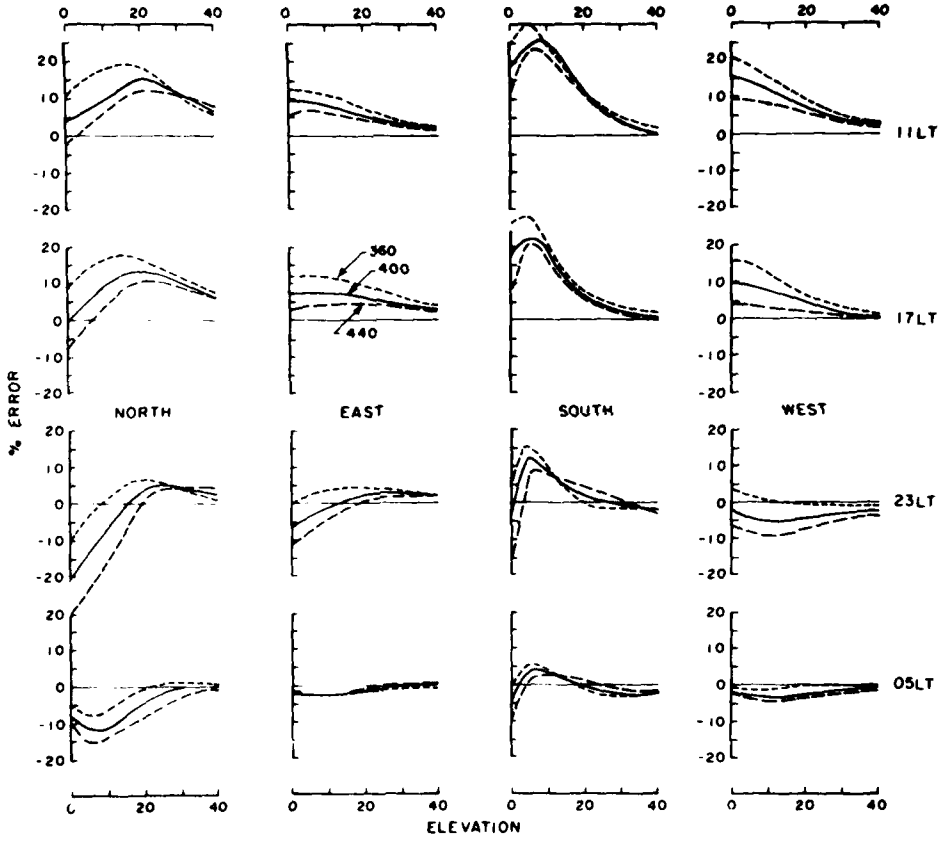

Figure 4. Variation of the Conversion Error With Elevation Angle for North, East, South, and West Azimuths, for Four Local Times (11, 17, 23, 05), and for Three Values of h_I, (360, 400 and 440 km) (Kwajalein, March, R = 100)

The other variations implicit in Figure 4 are discussed in the next section. The results discussed in the remainder of this report were obtained using h_I = 400 km. This seems a good average of the best values and is an appropriate height for F-region studies. For the results presented in Table 1, the average error is 4.7% for h_I = 400 km. It should be noted that the errors do not increase dramatically for other values of h_I—for the results presented in Table 1, the errors increase only to 5.5% for h_I = 360 and 440 km.

4. CONVERSION ERRORS FOR A LOW-LATITUDE STATION

Kwajalein (4.3° N, 167.5° E, 8.6° dip) lies between the crests of the equatorial anomaly and can be regarded here as a typical low-latitude station. The variation of the conversion errors for March, R = 100 have been given in Figure 4, for four azimuths and four local times. The errors are clearly greatest when looking north and south at low elevation angles. Figure 5 shows the errors for March, June, and December, for h_I = 400 km, and for R = 100, four azimuths and four local times. The errors are again greatest when looking north and south, the greatest values being for looking south in March during the day, exceeding 20%.

As might be expected, the errors are largest when there are large horizontal gradients of electron density along the observer-satellite path. Figure 6 shows the horizontal ranges (in degrees) at which a ray from the satellite will cut the ionosphere at a specified altitude, for elevation angles of 0 to 30°. Propagation is either north-south or south-north for this example since these azimuths correspond to the greatest errors. A ray at zero degrees, for example, will travel about 20° in latitude before encountering the ionosphere at 400 km. Figures 7a and 7b show how the ionosphere varies along the integration path for March, R = 100, h_I = 400 km, elevation = 10°, local time = 1100, which is when the conversion error has some of its highest values. It can be seen that under these conditions the ray passes right through a large part of the crests of the equatorial anomaly, indicating that it is the presence of the anomaly which cause the large errors. The errors are significantly lower for the east and west directions (Figure 5).

Evidence supporting the contention that it is horizontal gradients which cause the large errors is shown in Figure 8, which shows plots of percentage error versus gradient for the four azimuths (March, R = 100, elevation = 10°, h_I = 400 km). The gradients are represented by the change of $hmF2$ and $foF2$ over the height range of the first integral (200 to 400 km). Each data point is for a particular time of day from 0 to 22 UT, in steps of two hours. The two boxed values correspond to the data plotted in Figures 7a and 7b, and the straight lines are the least squares fit lines of error on gradient. The correlation coefficients are very high for north (0.97) and

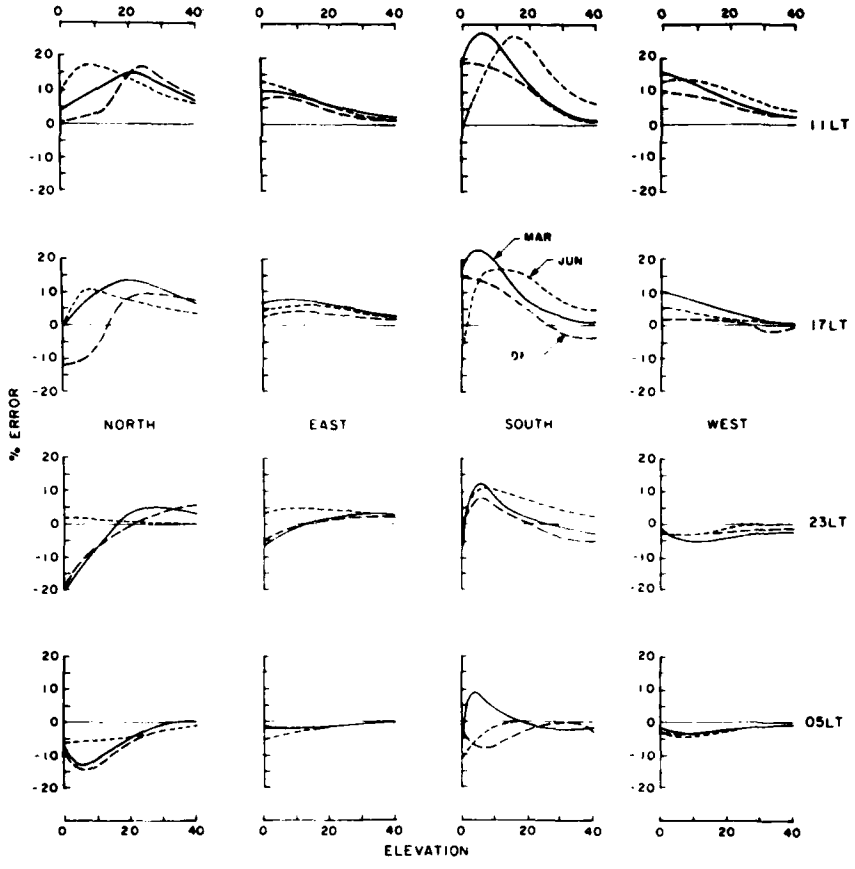

Figure 5. Variation of the Conversion Error With Elevation Angle for North, East, South, and West Azimuths, for Four Local Times (11, 17, 23, 05), and for Three Seasons (March, June and December) (Kwajalein R = 100, h_I = 400 km)

south (0.95) azimuths when the gradient in hmF2 is considered. For east and west azimuths, the correlations are lower, being 0.72 and 0.23, respectively. The correlations are much lower when the gradient in foF2 is considered, except for north azimuth, for which it is -0.87. The correlation for east azimuth increases from r = -0.40 to r = -0.85 if the two data points corresponding to dawn (0.5 and 0.7 LT) are ignored, suggesting that these two points represent a separate phenomenon (which they do).

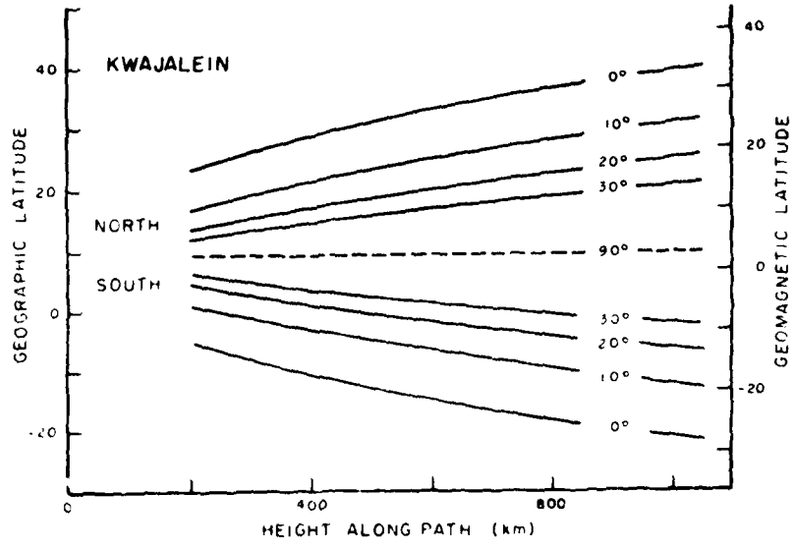

Figure 6. Latitudinal Coverage of the Ionosphere From Kwajalein, for Different Elevation Angles and Ionospheric Altitude

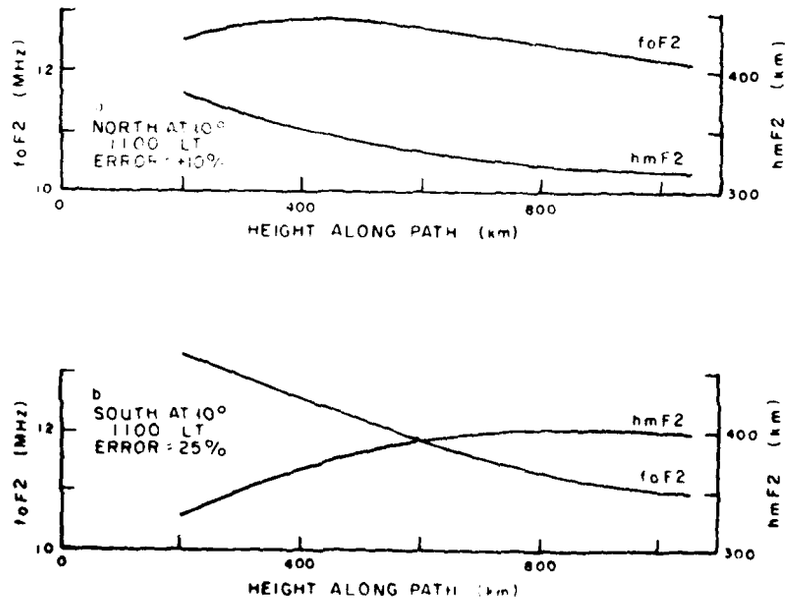

Figure 7. Variations of foF2 and hmF2 Along the Integration Path From Kwajalein for Two Times When the Conversion Error Had Some of its Highest Values, (March, R = 100, h_I = 400 km)

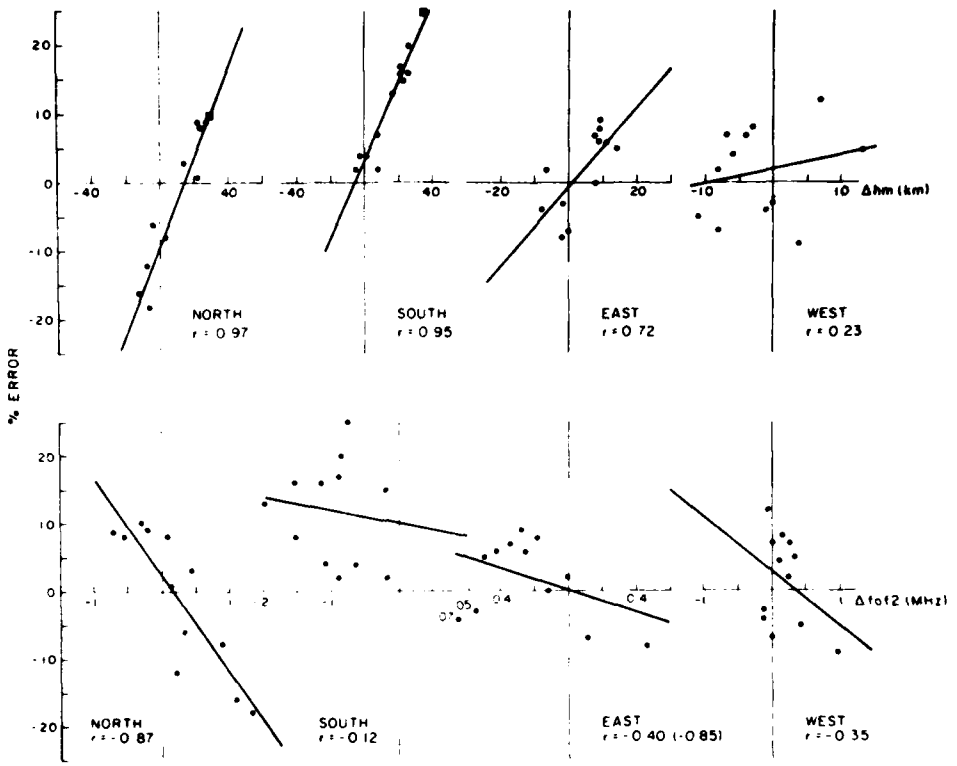

Figure 8. Variations of the Kwajalein Conversion Errors With Gradients in hmF2 (top panel) and foF2 (bottom panel), for North, South, East, and West Azimuths. The straight lines are the least squares fit regression lines and correspond to the linear correlation coefficients, r. (March, R = 100, Elevation = 10°)

The graphs of Figure 8 support the contention that the conversion errors are due to gradients along the path of hmF2 and foF2, especially the former. The correlation is most pronounced for north and south azimuths. The correlation with hmF2 may be explained qualitatively by noting that if hmF2 increases as the integration height increases, the same N(h) profile will, for a given altitude below hmF2, yield lower densities for the higher values of hmF2. It is difficult to be specific about the exact source of the conversion errors, because the net error is a result of cancellation between the errors above and below h_I, and each of these depends on the gradients in foF2 and hmF2.

5. CONVERSION ERRORS FOR A HIGH-LATITUDE STATION

Having found that the conversion errors at a low-latitude station are mainly due to the presence of horizontal gradients associated with the equatorial anomaly, it is logical to choose as a representative high-latitude station one which can "see" the main feature of the high-latitude ionosphere, the high-latitude trough. Consequently Goose Bay (53.3° N, 299.5° E, 65° N geomagnetic) has been chosen as a representative high-latitude station. Its position relative to the trough under certain conditions is shown in Figure 9.

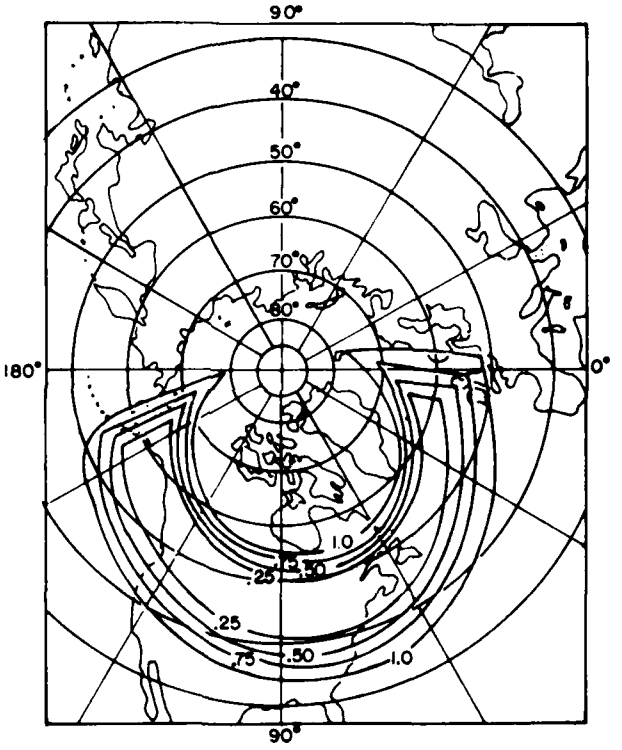

Figure 9. Location of the High Latitude Trough for Magnetically Quiet Conditions (March, R = 50, 06 UT), After Halcrow and Nisbet[4]

4. Halcrow, B.M., and Nisbet, J.S. (1977) A model of the F2 peak electron densities in the main trough region of the ionosphere, Radio Science, 12(5):815-820.

The range of latitudes which can be seen from Goose Bay is illustrated in Figure 10. (It should be noted here that the Bent model of the ionosphere is uncertain for very high latitudes.) Figures 11a and 11b show how hmF2 and foF2 vary along the integration paths for four azimuths (March, R = 100, h_I = 400 km, 0° elevation, 06 UT). The associated errors exceed 10% in all cases.

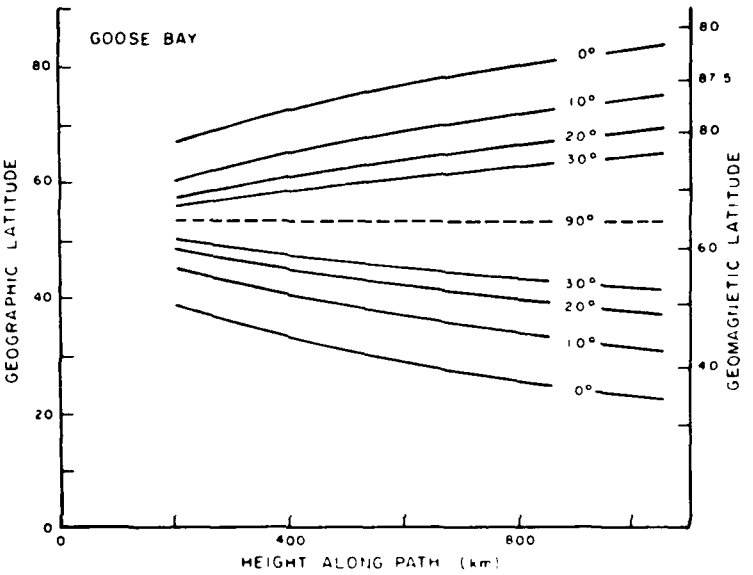

Figure 10. Latitudinal Coverage of the Ionosphere From Goose Bay, for Different Elevation Angles and Ionospheric Altitudes

The errors are shown as a function of azimuth, elevation angle, local time and season in Figure 12 (h_I = 400 km). In general, the major errors are for east, west and south propagation at around 02 LT, when the line of sight cuts some part of the trough. For north azimuth, the ionospheric part of the ray path lies north of the trough and the errors are somewhat smaller. There does not seem to be any simple relationship between the errors and gradients in either hmF2 or foF2.

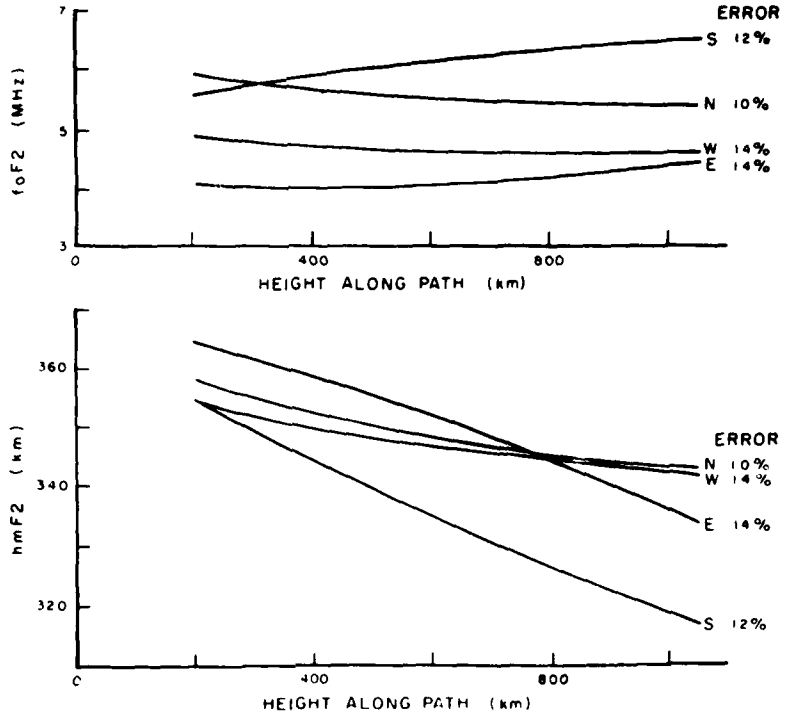

Figure 11. Variations of foF2 and hmF2 Along the Integration Path From Goose Bay for Four Azimuths, (March, R = 100, h_I = 400 km, 02 LT)

The conversion errors plotted in Figure 12 show a consistent positive bias, corresponding to sec I · TEC_v being too large. The bias could be removed to some extent by using a value of h_I greater than 400 km (smaller sec I). However, as indicated by Table 1, this is not an appropriate procedure for low solar activity, when a lower value of h_I (380 km) gives the smallest errors.

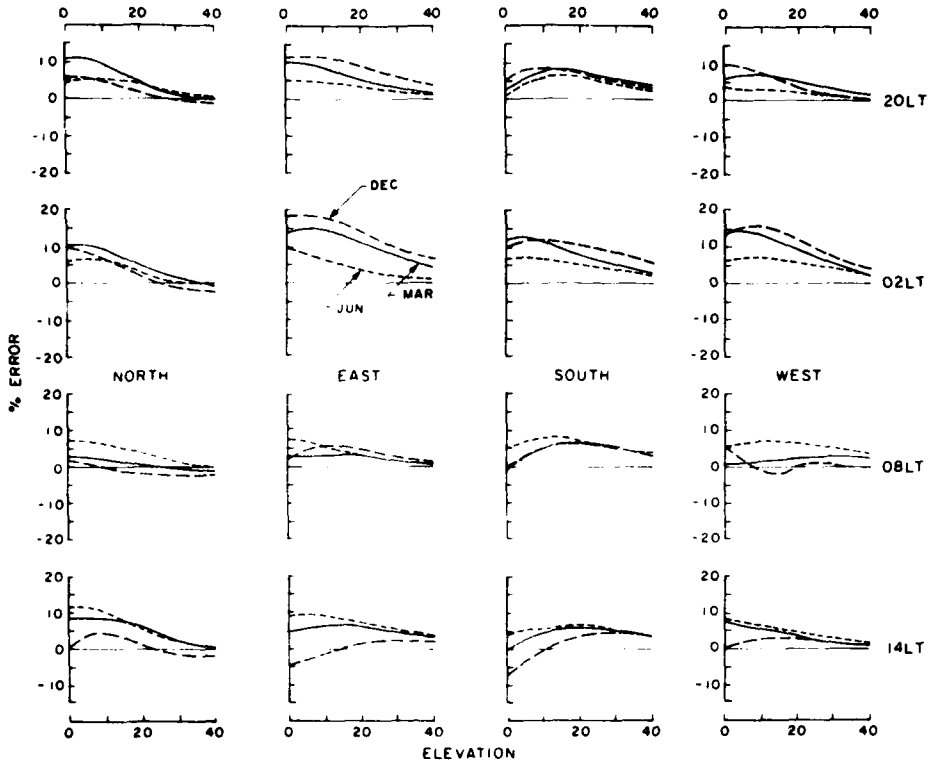

Figure 12. Variations of the Goose Bay Conversion Errors With Elevation Angle for North, East, South, and West Azimuths, for Four Local Times (20, 02, 08, 14) and for Three Seasons (March, June, December), (R = 100, h_I = 400 km)

6. CONVERSION ERRORS FOR A MID-LATITUDE STATION

Cape Canaveral (28.4° N, 279.4° E, 39.6° N geomagnetic) has been chosen as a typical mid-latitude station. The part of the ionosphere covered by looking north and south from Cape Canaveral is illustrated in Figure 13. Figures 14a and 14b correspond to the cases with largest errors (for March, R = 100, h_I = 400 km). The large error obtained looking south is a result of the ray passing through the northern crest of the equatorial anomaly, while the large error looking north is a result of the lowering of the ionosphere with increasing latitude.

The general correlation of the conversion error with gradients in hmF2 and foF2 is illustrated in Figure 15 (March, R = 100, h_I = 400 km, 0° elevation) for four azimuths. The gradients are represented by the changes of hmF2 and foF2 over the

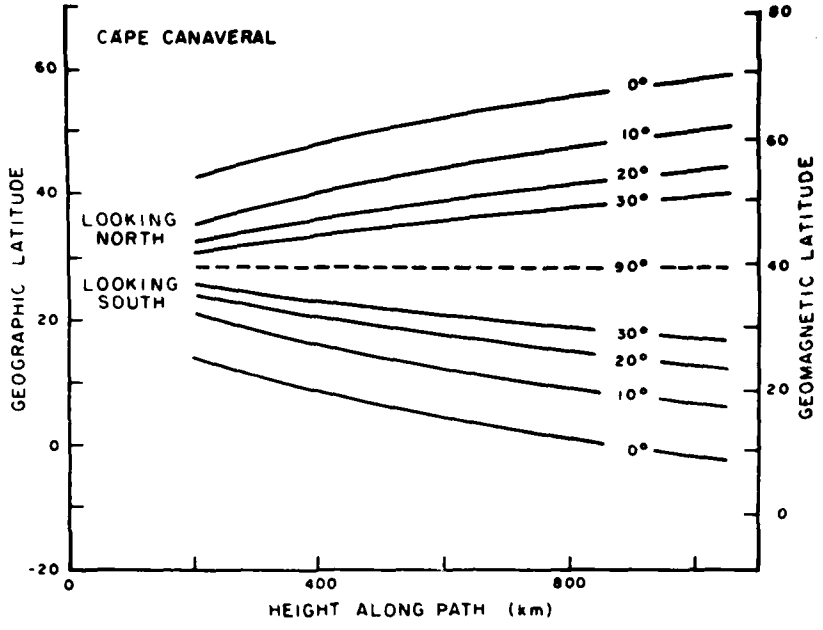

Figure 13. Latitudinal Coverage of the Ionosphere From Cape Canaveral for Different Elevation Angles and Ionospheric Altitudes

first integration range, while the azimuths are represented by the letters N, E, S and W. There are four data points (00, 06, 12, 18 UT) for each azimuth. The regression lines plotted are for all 16 data points and show a much higher correlation of error with the gradient in hmF2 ($r = 0.68$) than with foF2 ($r = -0.15$). Note that hmF2 changes by only 13 km at most (when looking south) in the 5 degrees of latitude encompassed by the first integration range. The correlation with the gradient in hmF2 is highest when looking south ($r = 0.89$) and lowest when looking west ($r = 0.20$). The boxed data points for south and north azimuth correspond to the cases shown in Figures 14a and 14b.

The conversion errors for Cape Canaveral are summarized in Table 2, which shows the smallest elevation angle for which the errors are less than 5% at 00, 06, 12 and 18 UT (LT = UT + 18.5), and the error corresponding to an elevation angle of 20°. Both of these levels are arbitrary, but reasonable choices. The parameter h_I has been set to 400 km, and the results are four azimuths, four times of day, three seasons, and two levels of solar activity.

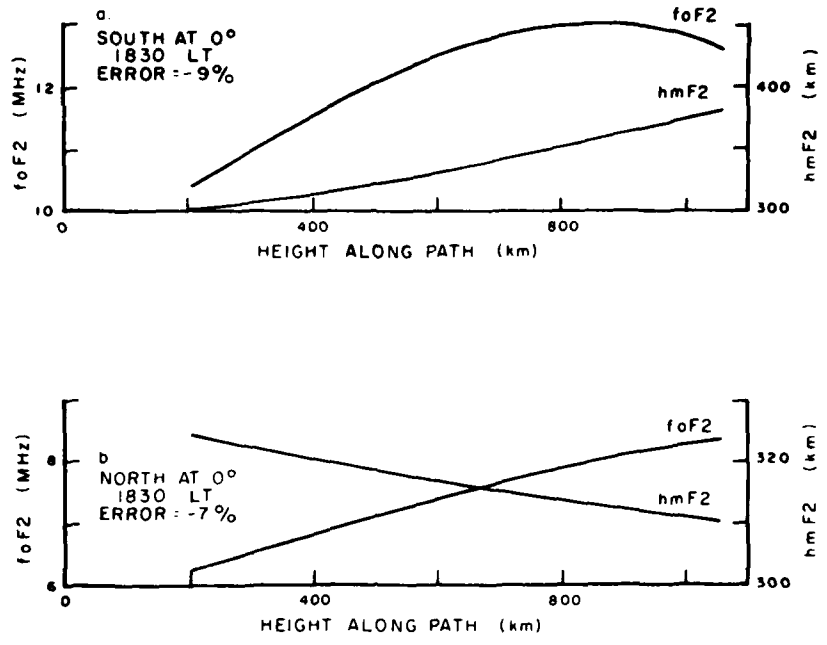

Figure 14. Variations of foF2 and hmF2 Along the Integration Path From Cape Canaveral for Two Times When the Conversion Error Was Fairly High, (March, R = 100, h_I = 400 km)

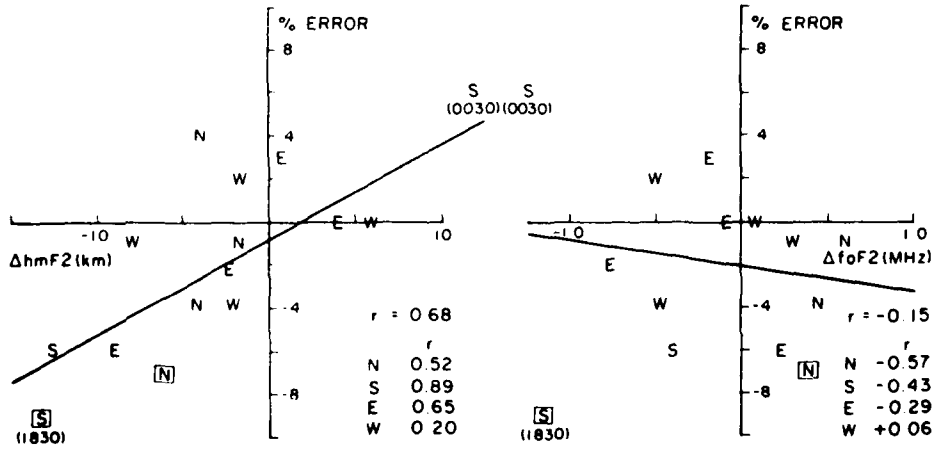

Figure 15. Variations of the Cape Canaveral Conversion Errors With Gradients in hmF2 and foF2, for North, South, East, and West Azimuths. The straight lines are the least squares fit regression lines and correspond to the linear correlation coefficients, r. (March, R = 100, h_I = 400 km, elevation = 0°). The boxed values correspond to the conditions of Figure 14

Table 2. Conversion Errors for Cape Canaveral Showing the Smallest Elevation Angle for Which the Error is Less Than 5% at 0, 06, 12 and 18 UT (LT = UT + 18.5), and the Error Corresponding to an Elevation Angle of 20°

		Elevation Angle at Which Error ≦ 5%					Error at 20° Elevation				
		0	90	180	270		0	90	180	270	
March	0	20	20	0	0		-3	-4	-1	-1	
R = 0	6	0	0	0	0		3	2	5	0	
	12	10	0	10	20		-1	2	0	4	
	18	0	0	0	0		-2	0	2	0	
R = 100	0	30	20	10	0		-5	-4	-1	0	
	6	0	0	40	0		-1	2	6	1	
	12	0	0	10	0		-3	3	0	-3	
	18	0	0	10	0		-2	1	-1	2	
											Aver.
						RMS	2.8	2.6	2.9	2.0	2.6
June	0	0	0	0	0		-2	-1	2	-1	
R = 10	6	0	0	40	0		5	0	7	1	
	12	0	0	0	0		1	1	3	0	
	18	0	0	0	0		1	1	0	2	
R = 100	0	0	0	10	0		-2	0	1	0	
	6	0	0	40	0		3	1	6	2	
	12	0	0	40	0		-1	1	5	1	
	18	0	0	0	0		-1	2	1	2	
											Aver.
						RMS	2.4	1.1	4.0	1.4	2.2
Dec	0	10	20	0	0		0	-4	0	2	
R = 10	6	0	0	10	0		2	2	3	0	
	12	20	0	10	30		-3	2	1	-5	
	18	10	20	20	10		-2	-3	-3	-2	
R = 100	0	20	20	0	0		-4	-4	-2	1	
	6	0	0	0	0		-4	2	4	1	
	12	20	30	10	20		-4	5	2	-4	
	18	20	10	30	10		-4	-2	-6	-1	
											Aver.
						RMS	3.2	3.2	3.1	2.5	3.0
						Aver.	2.8	2.3	3.0	2.0	

Consider first the elevation angles. A count of the number of times each elevation angle occurs in the table shows that elevation angles of 40° are required only when looking south (azimuth = 180°), and that all four cases occur at 06 or 12 UT (0030, 0630 LT). In the opposite sense, a zero elevation angle produces errors less than 5% on most occasions when looking west.

The variation of error with azimuth is better studied using the errors corresponding to an elevation angle of 20°, also shown in Table 2. RMS errors have been calculated for each azimuth and month (N = 8) and then averaged across the azimuth values for each month and across the months for each azimuth. It can be seen that the errors are greatest when looking south; greatest during December (winter); least when looking west; and least during June (summer). In general, the errors are lower when looking east or west than when looking north or south.

The conversion errors are also illustrated in Figure 16, which shows the variation of error with elevation angle for north, east, south and west azimuths, for four local times (19, 01, 07, 13), and for three seasons (March, June and December). The errors do not show the larger values attained near the equatorial anomaly (Figure 5) and high latitude trough (Figure 12) (R = 100, h_I = 400 km).

7. CONVERSION ERRORS FOR STATIONS AT 75° W

This section describes in a broad fashion the variation of the conversion error for stations at 285° E (75° W) and at latitudes of -10° to 70° (geomagnetic latitudes of ~ 1° and ~ 82° N). The results thus include the effects of the high-latitude trough and the equatorial anomaly, as well as illustrating the errors encountered when neither of these ionospheric features need be considered. The results are all for h_I = 400 km and R = 100, and are given separately for four azimuths. Table 3, for example, gives the results for March, and includes (a) the elevation angle required to be exceeded in order for the RMS error (averaged over the eight times 01, 04 ... 22 UT) to be ≤ 3%, or for all eight errors to be ≤ 5% in absolute values. Elevation angles between 20° and 50° inclusive are considered; (b) the RMS errors at 20° elevation. This elevation is a likely operational minimum set by antenna considerations; (c) the RMS errors at 30° elevation. This elevation would allow stations 10° apart to have overlapping fields of view.

Tables 4 and 5 give the corresponding results for June (summer) and December (winter). The three tables present no surprises and the broad picture is the same as that deduced from the results for Kwajalein, Cape Canaveral and Goose Bay: (a) the errors are least when looking east or west, except at high latitudes, where the trough is encountered; (b) for north and south azimuths, the errors are greatest when the trough and equatorial anomaly are encountered; (c) the general level of

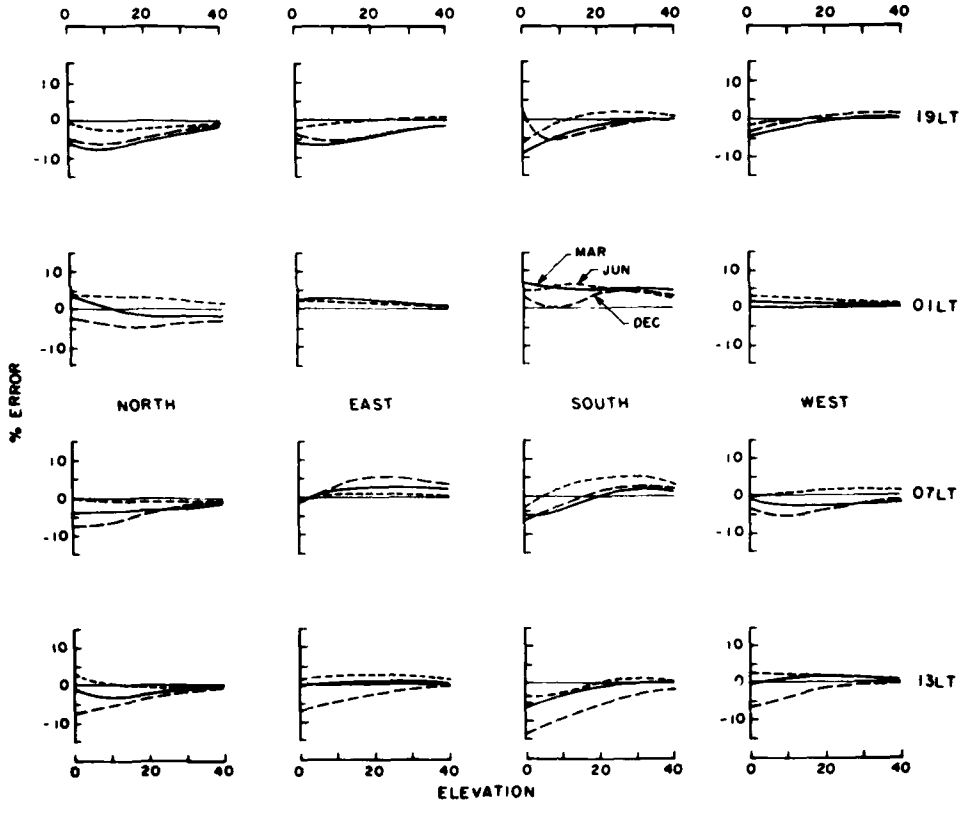

Figure 16. Variations of the Cape Canaveral Conversion Errors With Elevation Angle for North, East, South, and West Azimuths, for Four Local Times (19, 01, 07, 13) and for Three Seasons (March, June, December), (R = 100, h_I = 400 km)

error is greatest in December (winter) and least in June. Quantitative estimates of the errors may be obtained from the tables.

The use of RMS errors averaged over the eight local times hides any diurnal variation of the error which at times is very significant. Accordingly, the diurnal variation of the error has been plotted in Figures 17, 18 and 19 for each azimuth and station latitude and for March, June and December. The plots also show up any tendency for a systematic error to occur. The results shown are for R = 100, h_I 400 km and an elevation of 20°.

Table 3. Conversion Errors for Stations at 75° W in March, Showing (a) the Smallest Elevation Angles for Which the RMS Error Averaged Over the Eight Times (01, 04, ... 22 UT) is ≦ 3% or For All Eight Errors to be ≦ 5% in Absolute Value (Note that only elevation angles between 20° and 50° inclusive are considered); (b) the RMS Error at 20° Elevation; (c) the RMS Error at 30° Elevation. Errors are given for latitudes from -10° to 70° geographic and for North, East, South, and West azimuths. ($R = 100$, $h_I = 400$ km)

					RMS Errors at 20° El.				RMS Errors at 30° El.				
GG Lat	N	E	S	W	N	E	S	W	N	E	S	W	
70	40	40	40	40	5.1	7.0	8.7	8.6	3.9	4.3	5.6	5.2	
60	40	40	50	40	5.9	6.8	7.4	7.7	4.2	4.4	5.4	5.4	
50	20	30	40	40	2.5	4.3	6.3	5.3	1.4	2.6	5.0	3.7	
40	20	20	40	30	2.3	2.7	4.5	3.9	1.9	1.6	3.4	2.9	
30	30	20	40	20	3.6	2.4	4.1	3.0	2.7	1.4	3.2	2.1	
20	20	20	30	20	2.2	1.9	4.0	2.1	1.5	1.2	2.9	1.5	
15	20	20	40	20	2.4	1.6	5.4	2.0	2.0	1.1	3.6	1.4	
10	40	20	50	20	3.5	1.4	4.7	1.8	3.0	1.2	4.2	1.2	
5	50	20	40	20	5.3	1.6	2.5	1.9	4.8	1.2	2.9	1.2	
0	>50	20	30	20	7.3	2.4	6.1	2.1	5.8	1.7	2.4	1.2	
-5	>50	30	50	30	8.5	3.7	4.7	3.8	7.5	2.5	4.9	2.2	
-10	40	30	40	30	11.1	5.0	8.8	4.2	5.0	3.4	4.3	2.4	
									Aver. 3.64	2.22	3.98	2.53	Aver. 3.09
			(a)				(b)			(c)			

Table 4. Conversion Errors for Stations at 75° W in June, Showing (a) the Smallest Elevation Angle for Which the RMS Error Averaged Over the Eight Times (01, 04, ... 22 UT) is ≦ 3%, or for All Eight Errors to be ≦ 5% in Absolute Value (Note that only elevation angles between 20° and 50° inclusive are considered); (b) the RMS Error at 20° Elevation; (c) the RMS Error at 30° Elevation. Errors are given for latitudes from -10° to 70° geographic and for North, East, South, and West azimuths. (R = 100, h_I = 400 km)

					RMS Errors at 20° El.				RMS Errors at 30° El.				
GG Lat	N	E	S	W	N	E	S	W	N	E	S	W	
70	40	40	50	50	4.9	6.3	9.3	8.1	3.2	4.1	6.2	5.0	
60	40	40	50	50	5.2	5.8	7.4	7.5	3.3	3.8	5.5	5.2	
50	20	30	50	40	2.4	3.9	5.6	5.6	1.0	2.5	4.4	3.9	
40	20	20	20	30	1.5	2.5	2.8	3.7	0.7	1.7	2.2	2.7	
30	20	20	40	20	1.5	1.9	4.8	2.1	1.1	1.1	3.3	1.5	
20	20	20	20	20	2.0	1.5	2.8	1.5	1.7	1.1	2.4	1.1	
15	20	20	20	20	2.8	1.5	2.4	1.5	2.1	1.3	2.2	1.1	
10	30	20	20	20	3.5	1.8	1.7	2.0	2.9	1.5	2.0	1.3	
5	40	20	20	20	4.7	2.6	2.8	2.8	3.5	2.1	1.3	1.7	
0	40	30	40	30	5.3	3.4	6.1	3.3	3.7	2.5	3.4	2.0	
-5	30	30	40	20	4.0	3.9	7.6	2.9	3.0	2.8	3.5	1.8	
-10	50	30	50	20	4.5	3.9	15.4	2.5	3.2	2.8	9.7	1.7	
									Aver. 2.45	2.275	3.84	2.42	Aver. 2.75
		(a)				(b)				(c)			

Table 5. Conversion Errors for Stations at 75° W in December, Showing (a) the Smallest Elevation Angle for Which the Rms Error Averaged Over the Eight Times (01, 04, ... 22 UT) is ≦ 3%, or for All Eight Errors to be ≦ 5% in Absolute Value (Note that only elevation angles between 20° and 50° inclusive are considered); (b) the RMS Error at 20° Elevation; (c) the RMS Error at 30° Elevation. Errors are given for latitudes from -10° to 70° geographic and for North, East, South, and West azimuths. ($R = 100$, $h_I = 400$ km)

					RMS Errors at 20° El.				RMS Errors at 30° El.				
GG Lat	N	E	S	W	N	E	S	W	N	E	S	W	
70	30	50	50	50	3.7	9.7	10.8	10.3	2.7	6.4	7.3	6.4	
60	30	50	>50	50	3.7	8.6	8.6	8.9	2.9	5.7	6.8	6.3	
50	30	40	50	50	2.7	5.0	6.3	5.8	3.0	3.3	5.2	4.1	
40	30	30	40	40	3.7	3.3	4.7	4.4	3.0	2.1	3.6	3.2	
30	40	20	40	30	4.5	2.8	4.4	3.9	3.2	1.6	3.4	2.8	
20	30	20	30	30	3.1	2.4	3.5	3.3	2.0	1.5	2.5	2.1	
15	20	20	30	20	3.1	2.2	5.5	3.0	2.3	1.4	2.8	2.0	
10	40	20	40	20	3.9	2.2	7.4	2.9	3.2	1.4	5.5	1.8	
5	40	20	>50	20	5.8	2.0	5.0	2.9	4.4	1.4	5.4	1.8	
0	50	20	>50	20	7.6	2.2	7.9	2.6	5.5	1.4	3.8	1.7	
-5	>50	20	>50	20	6.8	2.4	7.9	2.5	5.6	1.8	5.2	1.4	
-10	>50	30	50	30	11.4	4.2	7.8	3.4	10.7	3.0	5.9	1.7	
									Aver. 4.04	2.58	4.78	2.94	Aver. 3.59
			(a)				(b)			(c)			

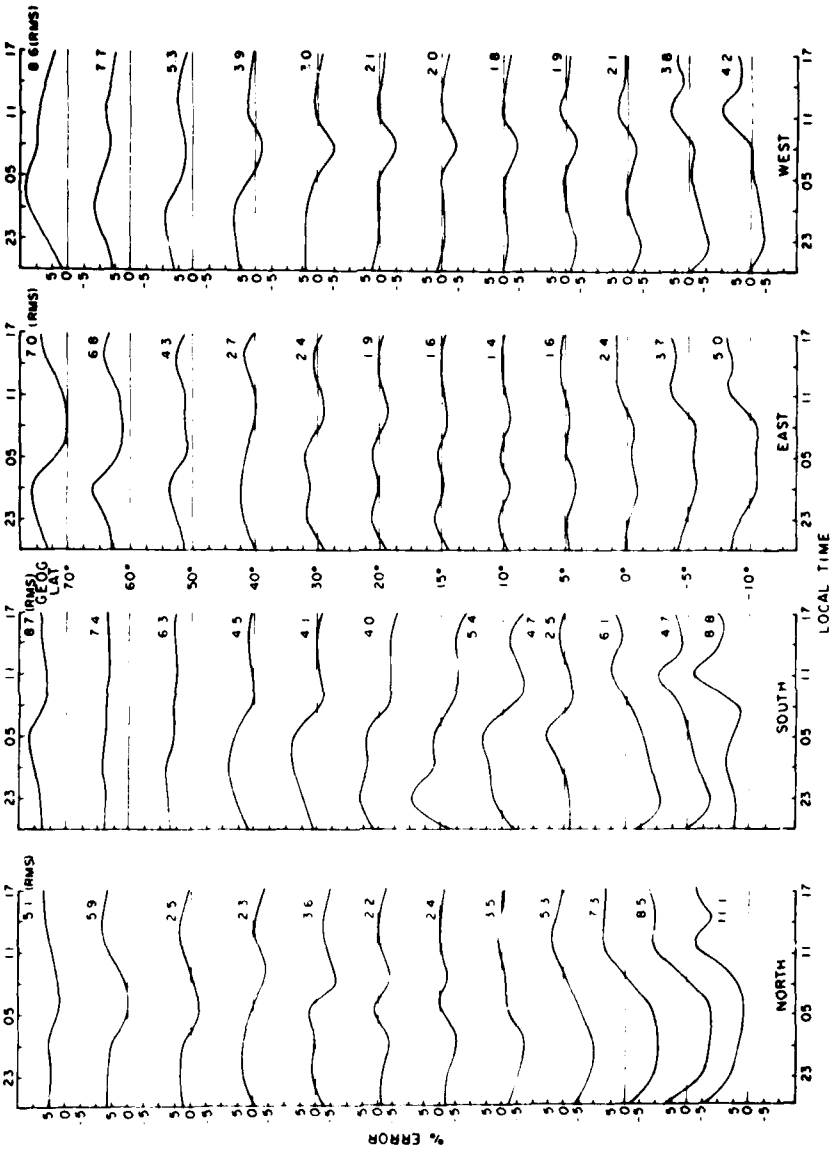

Figure 17. Diurnal Variations of the Conversions Errors for March for Stations at 75° W, as a Function of Latitude and Azimuth, (R = 100, h_I = 400 km, Elevation = 20°)

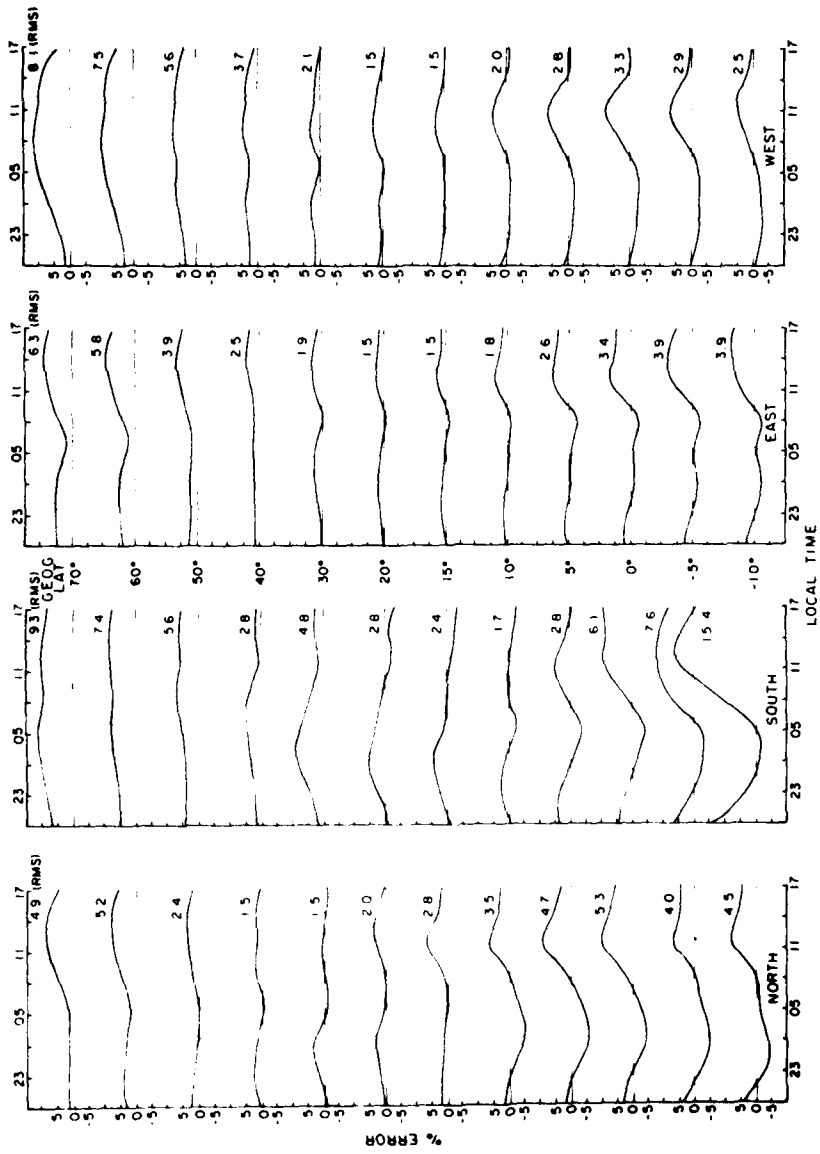

Figure 18. Diurnal Variations of the Conversion Errors for June for Stations at 75° W, as a Function of Latitude and Azimuth, (R = 100, h_I = 400 km, Elevation = 20°)

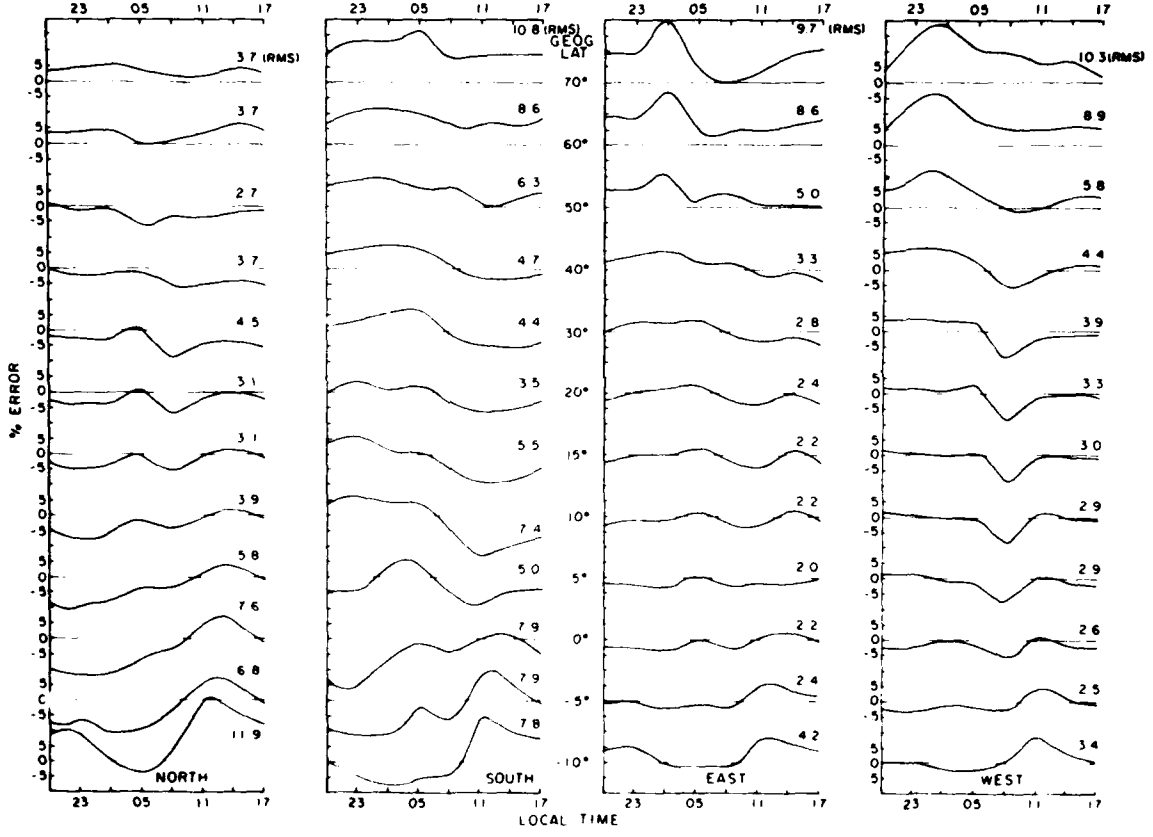

Figure 19. Diurnal Variations of the Conversion Errors for December for Stations at 75° W, as a Function of Latitude and Azimuth, (R = 100, h_1 = 400 km, Elevation = 20°)

The most significant diurnal variations occur for low-latitude observations affected by the equatorial anomaly (looking north or south in any month). Significant, but somewhat smaller variations are found for high-latitude stations affected by the high-latitude trough (for example, looking east or west in December). Systematic errors occur for a station at 10°S (geomagnetic latitude ~0°) when looking south in March and June, and in general for stations north of about 50°. Some of the systematic errors could be removed by a different choice of h_I.

A third source of gradients which might be expected to yield significant errors are the sunrise and sunset transitions, especially the former. Such errors are not obvious in the results although there are suggestions of dawn effects on some diurnal plots. For example, Figure 3 for h_I = 400 km does show a local change of error between 0400 and 0600 LT when looking east. Similar local increases can be seen in Figures 17 (March) and 19 (December) for station latitudes of -10° to 30°, looking east at 0500 LT, but not in Figure 18 (June).

The rapid morning increase of foF2 leads to significant gradients on paths looking west, resulting at times in noticeable errors. For example, the calculated values of TEC based on the vertical incidence value are too low near 08 LT in March and December (Figures 17 and 19). The errors result from a decrease in foF2 and an increase in hmF2 along the integration path, which looks towards earlier time zones.

8. DISCUSSION

The errors in the conversion of slant TEC to equivalent vertical incidence values have been found to vary with the elevation angle to the satellite, with the altitude at which sec I is evaluated, with the presence of ionospheric gradients along the ground-satellite path, and with the well-known variations of the ionosphere itself--diurnal, seasonal, solar cycle, and location. If the elevation angle is restricted to 20° or greater, the RMS errors averaged over a day are usually less than about 5% except where the ray path cuts either the equatorial anomaly or the high-latitude ionospheric trough. In general, the largest errors are encountered near the equatorial anomaly, where they can exceed 15% for an elevation angle of 20°. If elevation angles lower than 20° are considered, conversion errors in excess of 25% are possible near the anomaly, while errors of up to 20% are possible near the high-latitude trough.

There are several practical considerations associated with the errors in the conversion process. Consider firstly the situation of mid-latitude stations monitoring beacons on geostationary satellites at other longitudes. In such cases, the elevation angle can get very low, possibly resulting in non-negiligible conversion

errors. If the elevation angle gets down to 10°, a typical conversion error is 5% (Cape Canaveral, Figure 16), but can reach 10% for a fairly high mid-latitude station (Goose Bay, Figure 12, south azimuth). The error has a diurnal variation, which must also be taken into account. Changes of TEC less than 5 to 10% are not significant in such cases.

The next point to consider is the absolute size of the errors at different locations when the relative errors are the same. A 20% error at Goose Bay at 02 LT in December (R = 100) is equivalent to a change of TEC of $\sim 1.3 \times 10^{16}$ m^{-2}, whereas the same percentage error at Kwajalein at 17 LT in March (R = 100) is equivalent to a much larger change of $\sim 8 \times 10^{16}$ m^{-2}. In general, the absolute errors at low-latitude stations are higher than at high-latitude stations because of the higher electron densities involved.

The errors derived for low- and high-latitude stations apply only to the average behavior of the ionosphere under magnetically quiet conditions. Under disturbed geomagnetic conditions, the high-latitude trough expands equatorwards and a "mid-latitude" station can come under the trough and become a high-latitude station as far as TEC conversion errors are concerned. Similarly, under disturbed geomagnetic conditions, the poleward expansion of the crests of the equatorial anomaly is inhibited and a low-latitude TEC station will sample a significantly different section of the anomaly. Since it is not possible to model these and smaller day-to-day variations of the ionosphere and its gradients, the conversion errors associated with a location likely to become affected by such variations should be chosen pessimistically from those given in this report. In effect, the stations should be "moved" by an amount comparable to the amount by which the features of the ionosphere move. For the equatorial regions, this is about ± 10°. For high-latitude stations, account should be taken of how far equatorwards the high-latitude trough has expanded, which will depend directly on the level of magnetic activity.[4] The trough may in fact be recognizable on the TEC records if these yield sufficient spatial coverag .

The results presented in this report or obtained using further runs of the program SLANTEC may be used to estimate the ground-station separation required to yield acceptably small conversion errors. This spacing will change with latitude, and will also depend on what level of error is acceptable. A point which should be remembered is that even if the conversion errors are relatively large, say 20%, it may be better to make use of the data rather than simply rejecting them, because they do, after all, contain some useful information. In many cases, they will be the only such data available.

Finally, a word should be said about the applicability of the present results to real life. The results obtained and the conclusions drawn, are valid only in so far as the Bent ionospheric model is valid. While this model seems to be one of the best available for the present purposes, it predicts only a monthly average variation of the ionosphere for magnetically quiet conditions. Consequently it is recommended that the conversion errors discussed in this report be taken as lower limits when being applied to realtime observations of TEC.


DA
FIL